Talanta 83 (2010) 644–650

Contents lists available at ScienceDirect

Talanta

journal homepage: www.elsevier.com/locate/talanta

A new colorimetric chemodosimeter for Hg^{2+} based on charge-transfer compound of N-methylpyrrole with TCNQ

Paramjit Kaur[a,*], Sandeep Kaur[a,b], Yoganjaneyulu Kasetti[c], Prasad. V. Bharatam[c], Kamaljit Singh[b,*]

[a] Department of Chemistry, Guru Nanak Dev University, Amritsar, India
[b] Organic Synthesis Laboratory, Department of Applied Chemical Sciences and Technology, Guru Nanak Dev University, Amritsar, India
[c] Department of Medicinal Chemistry, National Institute of Pharmaceutical Education and Research (NIPER), S.A.S Nagar, India

ARTICLE INFO

Article history:
Received 3 September 2010
Received in revised form 7 October 2010
Accepted 8 October 2010
Available online 15 October 2010

Key words:
Charge-transfer
TCNQ
Colorimetric
Chemodosimeter
Mercury

ABSTRACT

Reaction of N-methylpyrrole and 7,7,8,8-tetracyanoquinodimethane (TCNQ) furnishes an intense blue unsymmetrical charge-transfer compound through regioselective attachment of tricyanoquinodimethane at the 2-position of N-methylpyrrole which was found to be selective chemodosimeter for Hg^{2+} ions in CH_3CN:H_2O mixture (1:1 *v*/*v*, pH = 7.0, 0.01 M HEPES, 0.15 M NaCl) as well as in the solid state when supported on silica, over a variety of metal ions. A plausible mechanism for the sensing process has been proposed and supported through the characterization of the resulting Hg^{2+} complex and the density functional theory (DFT) studies.

1. Introduction

Novel conjugated π-electron chromophores containing a donor and an acceptor have attracted considerable interest owing to their interesting properties and uses in a variety of high-tech applications such as near infrared (NIR) dyes [1] and non-linear optical (NLO) devices [2] owing to the inherent push-pull electronic effects in these molecules. Additionally, depending upon the strength of the covalently linked donor and acceptor components, strong intramolecular charge-transfer (ICT) transitions are facilitated, leading to intense colors of these compounds. The latter property has led to the design of several chemosensors involving charge-transfer [3] for the detection of a variety of ionic analytes and has been the subject of current research interest in our lab [4]. In the present investigation, we are reporting the synthesis of a new charge-transfer compound **2**, (Scheme 1), derived from N-methylpyrrole and 7,7,8,8-tetracyanoquinodimethane (TCNQ), as donor–acceptor combination. Considering the presence of soft electron rich centres in **2**, conducive for binding with soft metal centres, and the consequent perturbation of conjugation, we also report the application of **2** as chemodosimeter for the colorimetric detection of Hg^{2+} (Scheme 2). The mechanistic rationale, both for the formation of **2** as well as the sensing process is also unambiguously established.

The importance of selective detection of Hg^{2+} lies in the fact that Hg^{2+} pollution poses severe problems for human health and the environment [5]. Consequently, many methods have been developed to detect Hg^{2+} ion in the presence of its competitive cations. The techniques based on atomic absorption/emission spectroscopy and inductively coupled plasma mass spectrometry (ICPMS) for screening Hg^{2+} are limited by the cost factor in addition to the intricate sample preparations [6]. In contrast, simplified and straight forward methods for Hg^{2+} detection involving redox [7], chromogenic [8] and fluorogenic [9] changes invariably employ crown ethers [10], calix[4]arenes [11], cyclams [12], squaraines [13], thioureas [14], 1,3-dithiole-2-thione [15], 8-hydroxyquinolines [16], 1,4-disubstituted azines [7], fluoresceins [17], rhodamine lactam or thiolactam [18] etc. Inherent water solubility of several biomolecules such as proteins [19], oligonucleotides [20], DNAzymes [21] and antibodies [22] has allowed their use for the detection of Hg^{2+}. Colorimetric sensing of metal ions has been considered as advantageous in many respects and constitutes a dependable technique alongside fluorescence [7], however, reports on the use of colorimetric chemodosimeters which operate by a specific chemical reaction to generate a detectable chemical signal, for Hg^{2+} detection are scanty [23,24].

---

* Corresponding author. Tel.: +91 183 2258853; fax: +91 183 2258819 20.
E-mail addresses: paramjit19in@yahoo.co.in (P. Kaur), kamaljit19in@yahoo.co.in (K. Singh).

0039-9140/$ – see front matter © 2010 Elsevier B.V. All rights reserved.
doi:10.1016/j.talanta.2010.10.019

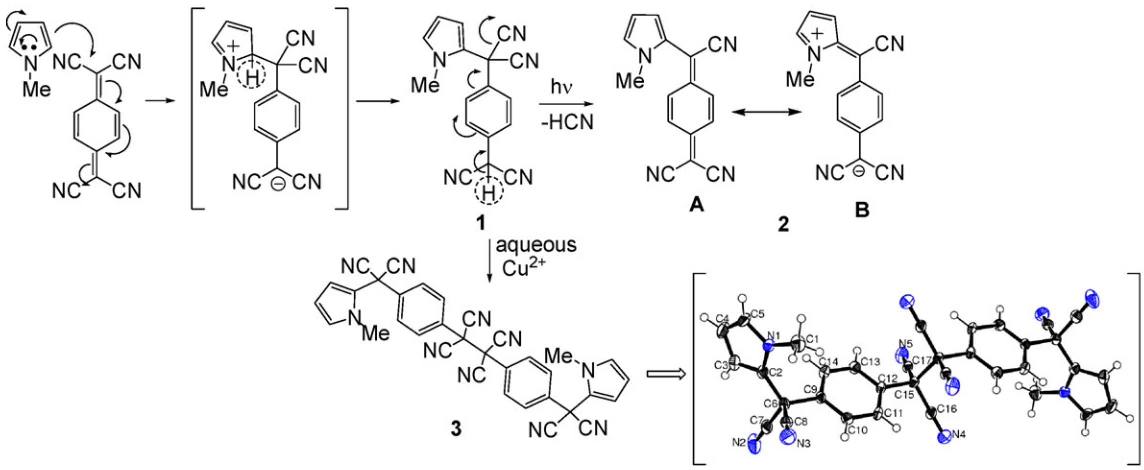

Scheme 1. Formation of blue charge-transfer compound **2** in the reaction of N-methylpyrrole and TCNQ. Inset: X-ray crystal structure of **3** (CCDC No. 760693).

2. Experimental

2.1. Chemicals

All reagents were purchased from Aldrich and were used without further purification. DCM was dried over benzophenone ketyl under inert atmosphere and distilled directly in the reaction flask. DMF was dried over a pinch of calcium hydride and distilled under reduced pressure over 4 Å molecular sieves. Silica gel G (60–120 mesh) was used for column chromatography.

2.2. Instrumentation

UV–vis spectra were recorded on a SHIMADZU 1601 PC spectrophotometer, with a quartz cuvette (path length, 1 cm) and studies were performed in AR grade CH_3CN and double distilled water. The cell holder of the spectrophotometer was thermostatted at 25 °C for consistency in the recordings. ^1H and ^{13}C NMR spectra were recorded on a JEOL-FT NMR AL 300 MHz and BRUKER Avance II 400 MHz spectrophotometer using $CDCl_3$ and DMSO-d_6 as solvent and tetramethylsilane ($SiMe_4$) as internal standard. Data are reported as follows: chemical shifts in ppm (δ), multiplicity (s = singlet, d = doublet, dd = doublet of doublet, m = multiplet), integration, coupling constant J (Hz) and assignment. The mass spectra were recorded with Esquire 3000–00037 mass spectrometer and Ultraflex/TOF/TOF mass spectrometer. Elemental analyses were performed with a Thermo Flash EA 1112 analyser and were within ± 0.4% of the theoretical values. IR spectrum was recorded on FT IR-SHIMADZU 8400 and Varian 660-IR Fourier-Transform spectrophotometers, in range 400–4000 cm^{-1}. Titration isotherms generated from UV–vis changes were fit in HypSpec [25] software to establish the stoichiometry of the complex and to determine the binding constant. The X-ray structure (CCDC No. 760693) was solved by direct methods using SIR 97 [26] and refined by full matrix least-square refinement techniques on F2 using SHELXTL [27].

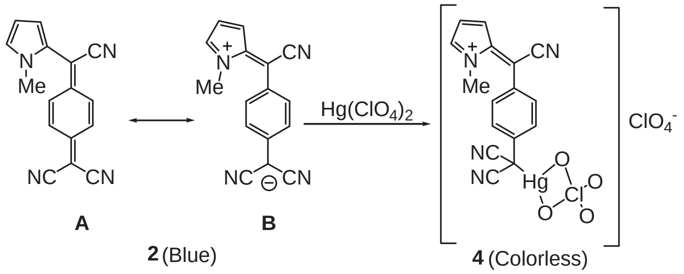

Scheme 2. Sensing of Hg^{2+} with **2**.

2.3. Computational Details

Ab initio DFT (density functional theory) studies [28] were carried out using Gaussion 03 software [29]. Initial optimization studies were carried out using semi-empirical PM3 method [30]. Resultant structures were subjected for optimization using B3LYP/LanL2DZ method. Partial atomic charges on the optimized structures were estimated using the NBO (natural bond orbital) method [31]. Electron density analysis has been carried out using the atoms in molecules (AIM) method [32] using the AIM2000 software [33].

2.4. Synthesis and characterization of compounds *1*, *2* and *3*

2.4.1. Synthesis of *1*

To freshly distilled N-methylpyrrole (0.5 g, 6 mmol) in anhydrous DMF (5.0 mL) a dilute solution of TCNQ (1.2 g, 6 mmol) dissolved in anhydrous DMF (150 mL) was added dropwise and the reaction mixture was stirred for 4 h at room temperature. After completion of the reaction, DMF was removed under reduced pressure on a rotary evaporator. The residue was washed with saturated aqueous sodium chloride solution and extracted with ethyl acetate (2 × 100 mL). The combined extract was dried over anhydrous sodium sulfate and the residue was chromatographed using hexane and its mixtures with ethyl acetate as eluent to obtain **1**, which was dissolved in anhydrous DCM (50 mL) and treated with charcoal (2 g). After filtration, the solvent was evaporated and the residue was recrystallized from DCM/hexane mixture to obtain **1** in the pure form (1.23 g, 70%). Mp: 90 °C; (Found: C, 71.20; H, 4.05; N, 24.15 $C_{17}H_{11}N_5$ requires C, 71.57; H, 3.89; N, 24.55%); ν_{max}/cm^{-1} 2060 (CN); δ_H (400 MHz; $CDCl_3$; Me_4Si) 3.47 (3H, s, NMe), 5.10 (1H, s, CH), 6.06–6.13 (2H, m, 2 × CH), 6.68–6.69 (1H, m, CH), 7.62 (4H, s, ArH); δ_C (300 MHz; $CDCl_3$; Me_4Si) 27.6, 35.1, 45.2, 108.0, 110.9, 112.9, 113.0, 119.5, 127.7, 128.5, 128.7, 134.4; m/z (EI): 283.6 (M^+−1), 256.6 (M^+−HCN-1).

2.4.2. Conversion of *1* to *2*

To isolate the blue charge-transfer compound **2**, **1** (1.0 g, 3.5 mmol) was dissolved in anhydrous CH_3CN (50 mL) or DMF (10 mL) and kept in direct sunlight or UV-light for 6 h. Solvent was removed under reduced pressure and the residue chromatographed to isolate **2** (0.36 g, 40%) alongwith **3** (an oxidatively coupled product) [34] (0.25 g, 27%).

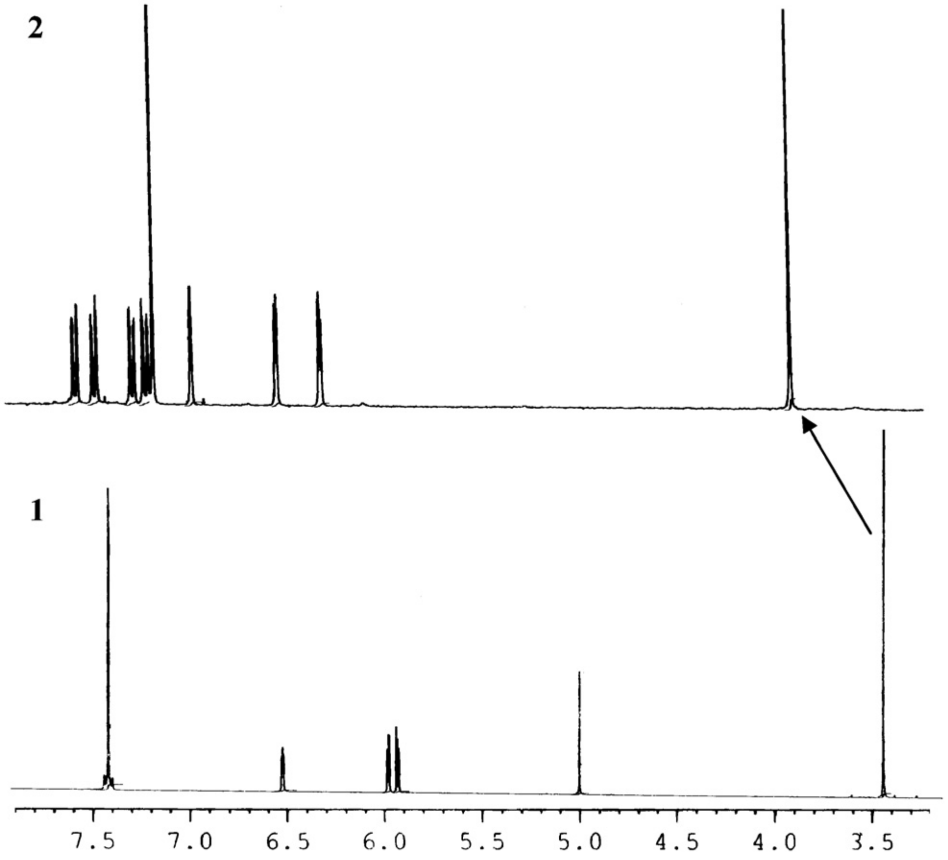

Fig. 1. ^{1}H NMR ($CDCl_3$) spectra of **1** and **2**.

2.4.3. *Compound **2***

Mp: 215 °C; (Found: C, 71.57; H, 3.65; N, 24.30 $C_{16}H_{10}N_4$ requires C, 71.82; H, 3.55; N, 24.63%); ν_{max}/cm^{-1} 2356 (CN); δ_H (400 MHz; $CDCl_3$; Me_4Si): 3.89 (3H, s, NMe), 6.37–6.38 (1H, m, CH), 6.60–6.62 (1H, m, CH), 7.06 (1H, d, *J* 1.6, CH), 7.29, 7.36 (1H, dd, *J* 1.8 and 1.8, CH), 7.31, 7.38 (1H, dd, *J* 1.8 and 1.9, CH), 7.56, 7.66 (1H, dd, *J* 1.9 and 1.9, CH), 7.58, 7.68 (1H, dd, *J* 1.9 and 1.9, CH); δ_C (400 MHz; $CDCl_3$; Me_4Si) 36.2, 77.2, 111.8, 111.9, 113.6, 113.7, 116.1, 122.6, 126.7, 126.9, 127.6, 133.1, 133.4, 134.0, 137.2, 153.0. DEPT−135 (400 MHz; $CDCl_3$; Me_4Si) (36.2, 77.2, 111.9, 122.6, 126.7, 126.9, 129.7, 133.1, 133.4, 134.0; *m*/*z* (EI): 257 (M^+-1).

2.4.4. *Compound **3***

Mp: 220 °C; (Found: C, 74.11; H, 3.92; N, 21.35 $C_{34}H_{20}N_{10}$ requires C, 74.40; H, 3.87; N, 21.70%); ν_{max}/cm^{-1} 2330 (CN); δ_H(400 MHz; DMSO; Me_4Si): 3.62 (6H, s, NMe), 6.15–6.18 (4H, m, 4 × CH), 6.83–6.84 (2H, m, 2 × CH), 7.78–7.88 (8H, m, ArH); δ_C (300 MHz; DMSO; Me_4Si) 34.7, 52.7, 54.9, 107.7, 108.7, 110.4, 112.3, 113.0, 118.9, 126.4, 128.1, 128.6, 130.1, 135.2; *m*/*z* (EI): 566.8 (M^+-1), 489.9 (M^+-1-N-methylpyrrole), 410.6 (489.9-N-methylpyrrole), 283.6 (M^+-285).

2.4.5. *Alternative synthesis of **3** involving oxidative coupling*

A solution of **1** (0.03 g, 0.1 mmol), $Cu_2(OAc)_4.2H_2O$ (0.021 g, 0.1 mmol) and DDQ (0.024 g, 0.1 mmol) in DCM (20 mL) was stirred at room temperature. The reaction completed (TLC) in 10 min. Solvent was removed and the residue was column chromatographed to isolate **3** (0.030 g, 50.8%).

2.5. *Isolation and characterization of complex **4***

To isolate the complex **4**, a solution of $Hg(ClO_4)_2{\cdot}xH_2O$ (0.077 g, 0.194 mmol) in distilled H_2O (5 mL) was added to a stirred solution of **2** (0.05 g, 0.194 mmol) in CH_3CN (5 mL). The reaction mixture was stirred at room temperature for 4 h. The resulting compound was filtered, washed with DCM/CH_3OH and dried to obtain complex **4** (0.068 g, 53.5%): Mp: > 260 °C; (Found C, 28.87; H, 1.50; N, 7.98, $C_{16}H_{10}N_4O_8Cl_2$ Hg requires C, 29.22; H, 1.50; N, 8.52%); ν_{max}/cm^{-1} 2171 (CN str), 2118 (CN str), 1112, 1084 (ClO_4 coordinated), 627 (ClO_4 uncoordinated), 553 (Hg–C) [35] *m*/*z* (EI): 679.94 ($M^+ + 23$).

(For copies of the NMR, IR, EI Mass, Fig. S1 in Supporting Information).

3. Results and discussion

3.1. *Reaction of N-methylpyrrole with TCNQ*

In order to investigate the mode of formation of charge-transfer compounds arising from the reaction of electron-rich heterocyclic species with TCNQ, we have carried out this study and reveal that the reaction of N-methylpyrrole with TCNQ proceeds exclusively at 2-position and forms an intense blue unsymmetrical charge-transfer covalent compound **2**, besides an oxidatively coupled product **3** (Scheme 1). Further confirmation of oxidative coupling mechanism involved in the conversion of **1** to **3** was achieved from the reaction of **1** with $Cu_2(OAc)_4{\cdot}2H_2O$ in the presence of DDQ [36]. Structure of **3** was solved by X-ray Crystallography (Scheme 1).

^{1}H NMR ($CDCl_3$) spectrum of **2** showed interesting features as the 3H singlet corresponding to N–Me signal shifted considerably downfield in comparison to **1**, to appear at δ 3.89 (Fig. 1) suggesting a strong intramolecular charge-transfer in the compound also indi-

Table 1
Solvatochromic data of the ICT band of **2** in selected solvents with solvatochromic parameter (π^*)[37].

Solvent†	π^*	Compound **2**	
		λ_{max} (nm)	ν_{max} (cm^{-1})
Tetrahydrofuran	0.58	552	18,115
Benzene	0.59	552	18,115
Acetone	0.71	554	18,050
Acetonitrile	0.75	559	17,889
Dichloromethane	0.82	564	17,730
Dimethylformamide	0.88	712	14,044
Dimethylsulfoxide	1.00	577	17,331

† Solvent used as received.

cated by the intense blue color. Thus **1** under the influence of light may lose a molecule of HCN to form tricyanoquinonoid derivative **2** as suggested in Scheme 1.

The UV–vis spectrum of **1** in acetonitrile showed an absorption band at 328 nm, while in the spectrum of **2**, an additional intense absorption at 559 nm was also observed. These bands are attributable to transitions ($\pi\pi^*$) to locally excited (LE) state and charge-transfer state ($n\pi^*$), respectively, owing to intramolecular charge-transfer from the pyrrole moiety to the tricyanoquinonoid moiety of **2**, as represented by the polar structure B (Scheme 1). A fair degree of solvatochromism (Table 1) was also observed as a consequence of change of solvent polarity attesting the stabilization of the polar excited state in polar solvents. In view of the fact that systems exhibiting strong ICT can undergo modulation of their ICT on binding with analytes, we explored the sensitivity of **2** with different metal ions. During our preliminary investigations, **2** was found to bind Hg^{2+} over other metal ions. Therefore, we performed the titration of **2** with Hg^{2+} and analyzed quantitatively.

3.2. UV–vis studies

The binding ability of **2** with Hg^{2+} was monitored by UV–vis experiments as the NMR technique was not found to be useful in view of considerable broadening of peaks during recording of NMR spectrum of **2** in the presence of Hg^{2+}. Change in the position as well as intensity of the ICT band allowed evaluation of the binding ability of the receptor **2** towards different cations. **2** was found to bind Hg^{2+}, selectively over a number of competitive cations, in $CH_3CN:H_2O$ (1:1, v/v) mixture. A solution of **2** (2×10^{-5} M) in buffered (pH 7.0, 0.01 M HEPES, 0.15 M NaCl) $CH_3CN:H_2O$ (1:1, v/v) mixture was found to give a stable blue solution [38] showing absorption bands at 316 (ε_{max} 13,735 l mol^{-1} cm^{-1}) and 572 nm (ε_{max} 30,735 l mol^{-1} cm^{-1}) (slightly shifted from 328 and 559 nm when recorded in pure acetonitrile owing to solvatochromism) and thus allowed the use of **2** for detection of analytes in mixed $CH_3CN:H_2O$ (1:1, v/v) mixture. The titration experiments were carried out by adding aliquots of different metal ions: Li^+, Na^+, Mg^{2+}, Ca^{2+}, Ba^{2+}, Mn^{2+}, Fe^{3+}, Fe^{2+}, Co^{2+}, Ni^{2+}, Ag^+, Hg^{2+}, Pb^{2+} as perchlorate salts, Cu^{2+}, Zn^{2+}, Cd^{2+} as nitrate salts, Al^{3+} as chloride salt and Cu^+ as iodide salt (Fig. 2) to the above solution of **2**. It was noted that upon addition of Hg^{2+} ions (0–60.0 equiv or even higher) to the solution of **2**, not only the absorption band at 572 nm disappears, the band at 316 nm gets red shifted ($\Delta\lambda = 34$ nm) to appear as a new band at 350 nm (ε_{max} 12,795 l mol^{-1}cm^{-1}). The process completes with concomitant color change of the solution from blue to almost colorless (Inset, Fig. 2) which is clearly visible to the naked eye. The other metal ions did not modulate the absorption spectrum of **2**. The color variation and selectivity of **2** over other cations are recorded in the Supporting Information (Figs. S2 and S3). The formation of new band at 350 nm, accompanied by quenching of internal charge-transfer process could be attributed to the interaction of **2** with $Hg(ClO_4)_2$ during the recognition process.

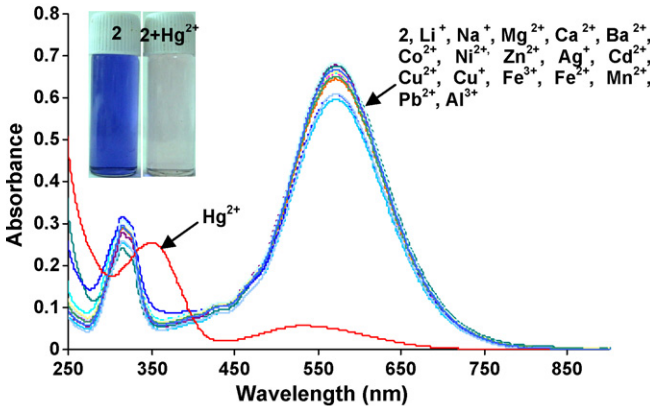

Fig. 2. Changes in the absorption spectrum of **2** [2×10^{-5} M in $CH_3CN:H_2O$ (1:1, v/v, pH 7.0, 0.01 M HEPES, 0.15 M NaCl)] after the addition of aqueous solution of Hg^{2+} and other metal ions (1.21×10^{-3} M) recorded immediately after mixing. Inset: Color change after the addition of Hg^{2+}.

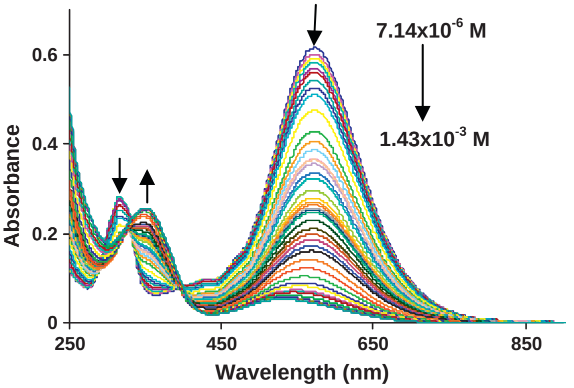

Fig. 3. Changes in the absorption spectrum of **2** [2×10^{-5} M in $CH_3CN:H_2O$ (1:1, v/v, pH 7.0, 0.01 M HEPES, 0.15 M NaCl)] upon titration with aqueous solution of Hg^{2+} (7.14×10^{-6} to 1.43×10^{-3} M).

Gradual change recorded in the absorption spectrum upon addition of different concentrations of Hg^{2+} to a solution of **2** during the titration is shown in Fig. 3. The change continued till 1.21×10^{-3} M concentration of Hg^{2+} was achieved beyond which no significant change was observed indicating the completion of the sensing process. The titration curve depicted two well defined isosbestic points at 328 and 398 nm conforming to a neat conversion of **2** into its adduct with Hg^{2+}. In Job's plot (Fig. 4), a maximum absorbance change was observed when the mole fraction of **2** versus Hg^{2+} was 0.5, which indicated the formation of 1:1 (**2**:Hg^{2+}) complex. Titra-

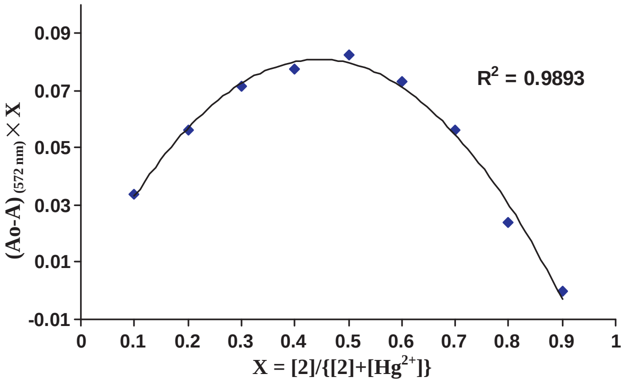

Fig. 4. Job's plot of a complex of **2** with Hg^{2+}.

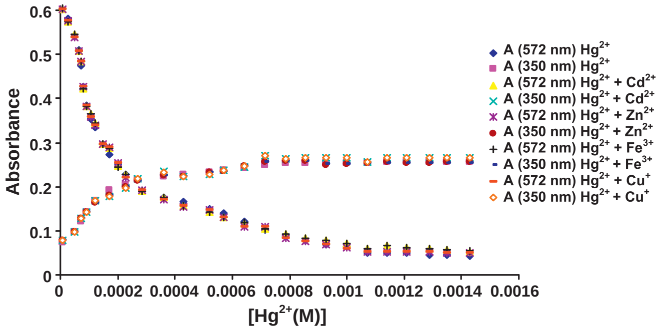

Fig. 5. Changes in the absorption spectrum of **2** [2×10^{-5} M in $CH_3CN:H_2O$ (1:1, *v*/*v*, pH = 7.0, 0.01 M HEPES, 0.15 M NaCl)] upon titration with aqueous solution of Hg^{2+} (1.21×10^{-3} M) in the presence of other metal ions (2.4×10^{-3} M).

tion data of **2** with Hg^{2+} was fitted using HypSpec [25] – a non-linear least-squares fitting programme. It allowed the establishment of the stoichiometry (1:1) of the most stable species (**2**: Hg^{2+}) present in the solution with the binding constant ($\log\beta$) = 3.945(2). Spectra were collected between 251 and 900 nm at 1 nm intervals. Analysis of data with Hypspec further allowed calculation of the molar absorptivity of **2**: [$\varepsilon_{\max}$ (572 nm, 316 nm) 35,000(400) l mol^{-1} cm^{-1} and 13260(370) l mol^{-1} cm^{-1}] and for the **2**:Hg^{2+} complex the value is 14,033(110) l mol^{-1} cm^{-1} (at 350 nm). These values represent a good correlation: 22 points, 650 wavelengths were fitted.

Resulted shift in the absorption band and change in color (blue to colorless) did not reverse upon the addition of concentrated solution of EDTA, demonstrating the irreversibility of the sensing process unlike many chemosensors [39] and thus the detection of Hg^{2+} by **2** could be visualized to proceed through an irreversible chemical reaction, rendering **2** as a unique Hg^{2+}-responsive charge-transfer chemodosimeter.

In order to check the selectivity of **2** in Hg^{2+} sensing and to rule out the possibility of interference from competitive cations, Hg^{2+} titration experiment of **2** was repeated in the presence of other cations: Zn^{2+}, Cd^{2+}, Fe^{3+} and Cu^{+}. Thus as shown in Fig. 5, during titration of **2** with Hg^{2+} in the presence of these ions, no significant variation in absorbance (at both wavelengths) was found by comparison with or without the competing metal ions. Therefore **2** could be envisioned to be capable of detecting Hg^{2+} in the competitive environment of the same group metal ions. The detection limit of **2** as a colorimetric sensor for the analysis of Hg^{2+} ions was found to be 10 ppm which is adequate for many types of chemical assays [40].

To explain the mode of binding of Hg^{2+} with **2**, we envisaged the formation of covalently linked species **4** through electrophilic substitution reaction of Hg^{2+} (Scheme 2) [24a].

The formation of **4** would also support the attendant “naked-eye” color change (blue to colorless) as a consequence of the quenching of intramolecular charge-transfer of **2**. Additional support to this hypothesis accrues from the fact that owing to the covalent attachment, **4** may not release Hg^{2+} to sequesterants such as EDTA, thus supporting the observed irreversibility in the recognition phenomenon. However, much like demercuration processes, the blue color of the **2** could be restored (matching UV–vis spectrum with original **2**) when the colorless solution obtained at the end of the sensing experiment was treated with $NaBH_4$ [41]. Further, in order to support the proposed sensing process, the complex **4** was isolated and fully characterized by IR, mass spectroscopic techniques (Fig. S1 in Supporting Information) as well as microanalytical data. However, owing to poor solubility of **4**, NMR (^{1}H and ^{13}C) spectra could not be recorded.

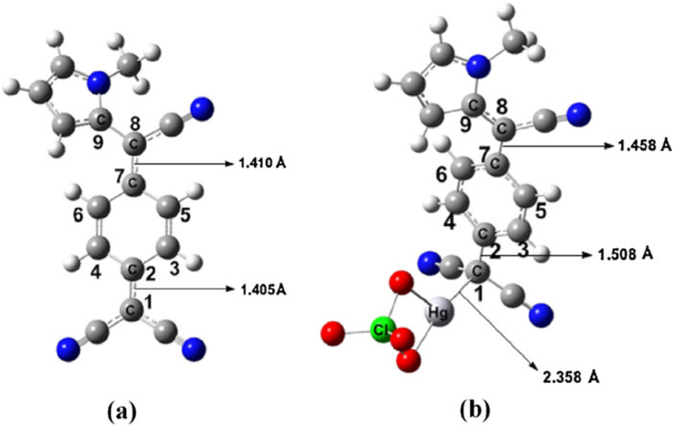

Fig. 6. 3D structures of **2** (a) and **4** (b) obtained using B3LYP/LanL2DZ optimization.

3.3. *Density functional theory (DFT) studies*

Quantum chemical calculations were carried out on molecules **2** and **4** so as to obtain their geometrical details, to understand the charge-transfer phenomenon and to analyze the electronic characteristics of these systems. Fig. 6 shows the 3D structures of **2** and **4** along with a few geometrical parameters obtained using B3LYP/LanL2DZ calculations.

In **2**, the C1–C2 bond length is 1.405 Å, which represents a partial double bond character. Similarly the C7–C8 bond is also a partial double bond with a bond length 1.410 Å. The C8–C9 bond length is also corresponding to a partial C–C double bond. Even the ring C–C bond lengths represent partial double bond character, indicating that the geometrical parameters of **2** represent a true resonance hybrid of structures **2A** and **2B**. Upon complexation with $Hg(ClO_4)_2$, the C1–C2 and the C7–C8 bond lengths get elongated and the C8–C9 bond length get shortened in **4**. Also, the ring C–C bonds get aromatic C–C character. All these facts indicate that there is a clear shift of the structure towards **2B** upon reaction with Hg^{2+}. The Hg–C1 distance in **4** is 2.358 Å, clearly indicating that in **4**, the Hg–C1 interaction is of covalent nature [42,43]. Estimated NBO charge on the N-methylpyrrole unit in the neutral molecule is −0.207 (Table 2). In **2**, the charge on the same unit is strongly positive 0.226 showing a shift of 0.433 units of electronic density from the N-methylpyrrole ring to the rest of the molecule. In the mercury complex **4**, the charge-transfer from the N-methylpyrrole ring to the rest of the molecule is 0.847. Besides this, the partial atomic charge on the nitrogen atom of the simple N-methylpyrrole ring −0.421 which is slightly reduced to −0.405 in **2** and further reduced to −0.384 in **4**. NBO charge analysis and their results indicated that N-methylpyrrole ring system of **2** is gaining overall positive charge when compared to simple N-methylpyrrole ring and the positive charge is further increased after complexation with mercury which is attached with one perchlorate (in **4**). In molecule **2**, the electron density (ρ) across C1–C2 bond is 0.286 and the ellipticity (ε) value is 0.2, indicating a weak double bond across these two atoms (AIM analysis). In molecule **4**, the electron density across C1–C2 is slightly reduced but ellipticity (ε) is drastically reduced indicating the formation of a regular single bond

Table 2
Partial atomic charges on Nitrogen and N-methylpyrrole rings obtained using Natural Bond Orbital (NBO) method.

NBO charges	N-methylpyrrole	**2**	**4**
Charge on Nitrogen	−0.421	−0.405	−0.384
Overall charge on N-methylpyrrole ring	−0.207	0.226	0.640

Table 3
Electron density analysis in **2** and **4** in comparison to that of dimethylmercury and methylmercury perchlorate.

Parameter	2	4		Me_2Hg	$MeHgClO_4$
	C1–C2	C1–C2	Hg–C1	Hg–C	Hg–C
Bond length (Å)	1.405	1.508	2.358	2.241	2.215
$\boldsymbol{\rho}$	0.286	0.237	0.067	0.084	0.084
$\nabla^2\boldsymbol{\rho}$	−0.748	−0.504	0.108	−0.128	0.120
ε	0.2	0.077	0.016	0.93E-5	0.014

$\boldsymbol{\rho}$ = Electron Density, $\nabla^2\boldsymbol{\rho}$ = Laplacian of ρ (The Laplacian of the electron density ρ determines where electron density is locally concentrated, $\nabla^2\rho(r) < 0$, and locally depleted, $\nabla^2\rho(r) > 0$), $\boldsymbol{\varepsilon}$ = Ellipticity (Ellipticity of the bond provides a measure of the extent to which charge is referentially accumulated in a given plane. Increased ellipticity may reflect an increase in structural instability or in the π character of a certain bond).

across these two atoms. A bond critical point was observed between Hg–C1 in **4** indicating the presence of a regular bond between these two atoms. The ρ, $\nabla^2\rho$ and ε values across the Hg–C1 bond in **4** are 0.067, 0.108 and 0.016, respectively which are quite comparable to those of methylmecury perchlorate (0.084, 0.120 and 0.014, respectively) and dimethylmercury (0.084, 0.128 and 0.93E-5). This comparative analysis indicates that the Hg–C1 bond in **4** should be considered as a regular covalent bond between Hg and C1. Moreover, the estimated Hg–C1 bond length in **4** (2.358 Å) is only 0.143 Å longer than that of methylmecury perchlorate (2.215 Å) and 0.117 Å longer than that of dimethylmercury. All these factors support the regular single bond character across Hg–C1 in **4** (Table 3) (Fig. S6 in Supporting Information).

4. Practical application

The sensing of Hg^{2+} by **2** worked also when it was supported on silica. Thus, a solution of **2** in CH_3CN (2 mL, 2×10^{-5} M, 4×10^{-8} mol) was added to silica (60–120 mesh, 0.1 g, colorless), stirred for 1 min and the solvent was removed to get purple silica (Fig. 7) which was treated with a solution of Hg^{2+} (2 mL, 1.21×10^{-3} M, 2.42×10^{-6} mol) in double distilled water. An instant color change from purple to colorless was noticed. Solvent was removed under reduced pressure and silica dried in oven to obtain colorless silica. Since the color change was rapid and clearly detected, the sensor **2** can be used for practical applications [24b].

5. Conclusion

In summary, we have explored the reaction of TCNQ with N-methylpyrrole and established the formation of a new charge-transfer compound. The strong intramolecular charge-transfer allowed it to be used as an efficient, highly selective and reasonably sensitive colorimetric chemodosimeter for the detection of Hg^{2+} from mixed $CH_3CN:H_2O$ (1:1, v/v) mixture as well as in the solid state when supported on silica.

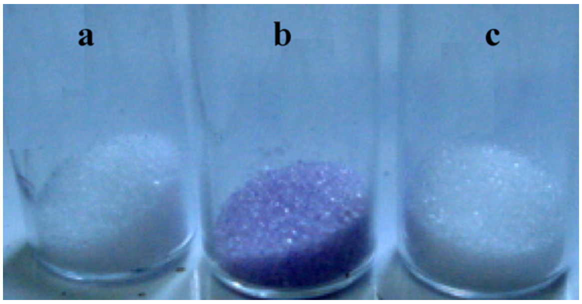

Fig. 7. Observed color changes in solid state: untreated silica (a), **2** supported on silica (b) and **2** after treatment with Hg^{2+} (c).

Acknowledgements

PK and KS thank UGC [F. 32-223/2006 (SR)] and CSIR [01(2265)/08-EMR (II)], New Delhi for financial assistance. SK is grateful to CSIR, New Delhi for senior research fellowship.

Appendix A. Supplementary data

Supplementary data associated with this article can be found, in the online version, at doi:10.1016/j.talanta.2010.10.019.

References

[1] (a) G. Qian, B. Dai, M. Luo, D. Yu, J. Zhan, Z. Zhang, D. Ma, Z.Y. Wang, Chem. Mater. 20 (2008) 6208–6216;
(b) G.M. Fischer, M. Isomaki-Krondahl, I. Gottker-Schnetmann, E. Daltrozzo, A. Zumbusch, Chem. Eur. J. 15 (2009) 4857–4864.
[2] (a) L.R. Dalton, P.A. Sullivan, D.H. Bale, Chem. Rev. 110 (2010) 25–55;
(b) S.R. Marder, Chem. Commun (2006) 131–134;
(c) R.M. Blanca, Engineering of Crystalline Materials Properties, Springer, Netherlands, 2007, pp. 375.
[3] (a) M. Beija, C.A.M. Afonso, J.M.G. Martinho, Chem. Soc. Rev. 8 (2009) 2410–2433;
(b) E. Ranyuk, C.M. Douaihy, A. Bessmertnykh, F. Denat, A. Averin, I. Beletskaya, R. Guilard, Org. Lett. 11 (2009) 987–990.
[4] (a) P. Kaur, S. Kaur, K. Singh, Tetrahedron Lett. 48 (2007) 7191–7193;
(b) P. Kaur, S. Kaur, A. Mahajan, K. Singh, Inorg. Chem. Commun. 11 (2008) 626–629;
(c) P. Kaur, S. Kaur, K. Singh, Inorg. Chem. Commun. 12 (2009) 978–981;
(d) P. Kaur, D. Sareen, S. Kaur, K. Singh, Inorg. Chem. Commun. 12 (2009) 272–275;
(e) P. Kaur, D. Sareen, Dyes Pigm. 88 (2011) 296–300.
[5] (a) H.H. Harris, I. Pickering, G.N. George, Science 301 (2003) 1203;
(b) E.M. Nolan, S.J. Lippard, Chem. Rev. 108 (2008) 3443–3480;
(c) Mercury update: Impact on Fish Advisories, EPA Fact Sheet EPA-823-F-01-011, EPA, Office of Water, Washington, DC, 2001.
[6] E. Curdova, L. Vavruskova, M. Suchanek, P. Baldriam, J. Gabriel, Talanta 62 (2004) 483–487.
[7] A. Caballero, R. Martinez-manez, V. Lloveras, I. Ratera, J. Vidal-Gancedo, K. Wurst, A. Tarraga, P. Molina, J. Veciana, J. Am. Chem. Soc. 127 (2005) 15666–15667.
[8] (a) A. Caballero, A. Espinosa, A. Tarraga, P. Molina, J. Org. Chem. 73 (2008) 5489–5497;
(b) T. Romero, A. Caballero, A. Espinosa, A. Tarraga, P. Molina, Dalton Trans. (2009) 2121–2129.
[9] (a) H. Lu, L. Xiong, H. Liu, M. Yu, Z. Shen, F. Li, X. You, Org. Biomol. Chem. 7 (2009) 2554–2558;
(b) M. Tian, H. Ihmels, Chem. Commun. (2009) 3175–3177.
[10] M. Zhu, M. Yuan, X. Liu, J. Xu, J. Lv, C. Huang, H. Liu, Y. Li, S. Wang, D. Zhu, Org. Lett. 10 (2008) 1481–1484.
[11] A.B. Othman, J.W. Lee, J.S. Wu, J.S. Kim, R. Abidi, P. Thuery, J.M. Strub, A.V. Dorsselear, J. Vicens, J. Org. Chem. 72 (2007) 7634–7640.
[12] S.H. Kim, J.S. Kim, S.M. Park, S.K. Chang, Org. Lett. 8 (2006) 371–374.
[13] J.V. Ros-Lis, R. Martinez-manez, K. Rurack, F. Sancenon, J. Soto, M. Spieles, Inorg. Chem. 43 (2004) 5183–5185.
[14] B. Liu, H. Tian, Chem. Commun. (2005) 3156–3158.
[15] G. Zhang, D. Zhang, S. Yin, X. Yang, Z. Shuaia, D. Zhu, Chem. Commun. (2005) 2161–2163.
[16] K.G. Vaswani, M.D. Keranen, Inorg. Chem. 48 (2009) 5797–5800.
[17] H.J. Kim, J.E. Park, M.G. Choi, S. Ahn, S.-K. Chang, Dyes Pigm. 84 (2010) 54–58.
[18] (a) W. Huang, C. Song, C. He, G. Lv, X. Hu, X. Zhu, C. Duan, Inorg. Chem. 48 (2009) 5061–5072;
(b) M.H. Lee, J.S. Wu, J.W. Lee, J.H. Jung, J.S. Kim, Org. Lett. 9 (2007) 2501–2504;
(c) H. Yang, Z. Zhou, K. Huang, M. Yu, F. Li, T. Yi, C. Huang, Org. Lett. 9 (2007) 4729–4732;

(d) X.Q. Zhan, Z.H. Qian, H. Zheng, B.Y. Su, Z. Lan, J.G. Xu, Chem. Commun. (2008) 1859–1861.

[19] S.V. Wegner, A. Okesli, P. Chen, C. He, J. Am. Chem. Soc. 129 (2007) 3474–3475.

[20] A. Ono, H. Togashi, Angew. Chem. Int. Ed. 43 (2003) 4300–4302.

[21] J.M. Thomas, R. Ting, D.M. Perrin, Org. Biomol. Chem. 2 (2004) 307–311.

[22] M. Matsushita, M.M. Meijler, P. Wirsching, R.A. Lerner, K.D. Janda, Org. Lett. 7 (2005) 4943–4946.

[23] W. Liu, L. Xu, H. Zhang, J. You, X. Zhang, R. Sheng, H. Li, S. Wu, P. Wang, Org. Biomol. Chem. 17 (2009) 660–664.

[24] (a) M.G. Choi, D.H. Ryu, H.L. Jeon, S. Cha, J. Cho, H.H. Joo, K.H. Hong, C. Lee, S. Ahn, S.-K. Chang, Org. Lett. 10 (2008) 3717–3720;
(b) O. Campo, A. Carbayo, J.V. Cuevas, A. Munoz, G. Garcıa-Herbosa, D. Moreno, E. Ballesteros, S. Basurto, T. Gomez, T. Torroba, Chem. Commun. (2008) 4576–4578;
(c) M.G. Choi, Y.H. Kim, J.E. Namgoong, S.-K. Chang, Chem. Commun. (2009) 3560–3562;
(d) M.H. Lee, S.W. Lee, S.H. Kim, C. Kang, J.S. Kim, Org. Lett. 11 (2009) 2101–2104.

[25] P. Gans, A. Sabatini, A. Vacca, Talanta 43 (1996) 1739–1753.

[26] A. Altomare, G. Cascarano, C. Giacovazzo, A. Gualardi, App. Crystallogr. 26 (1993) 343–350.

[27] G.M. Sheldrick, *SHELXTL-PC* Version 5.05, in: Structure Determination Programs, Siemens Ana. Instruments Inc, Madison. WI, 1995.

[28] (a) R.G. Parr, W. Yang, Density Functional Theory of Atoms and Molecules, Oxford University Press, New York, 1989;
(b) L.J. Bartolotti, K. Fluchick, in: K.B. Lipkowitz, D.B. Boyd (Eds.), Reviews in Computational Chemistry, 7, VCH Publishers, New York, 1996, p. 187.

[29] M.J. Frisch, G.W. Trucks, H.B. Schlegel, G.E. Scuseria, M.A. Robb, J.R. Cheeseman, J.A. Montgomery, T. Vreven Jr., K.N. Kudin, J.C. Burant, J.M. Millam, S.S. Iyengar, J. Tomasi, V. Barone, B. Mennucci, M. Cossi, G. Scalmani, N. Rega, G.A. Petersson, H. Nakatsuji, M. Hada, M. Ehara, K. Toyota, R. Fukuda, J. Hasegawa, M. Ishida, T. Nakajima, Y. Honda, O. Kitao, H. Nakai, M. Klene, X. Li, J.E. Knox, H.P. Hratchian, J.B. Cross, C. Adamo, J. Jaramillo, R. Gomperts, R.E. Stratmann, O. Yazyev, A.J. Austin, R. Cammi, C. Pomelli, J.W. Ochterski, P.Y. Ayala, K. Morokuma, G.A. Voth, P. Salvador, J.J. Dannenberg, V.G. Zakrzewski, S. Dapprich, A.D. Daniels, M.C. Strain, O. Farkas, D.K. Malick, A.D. Rabuck, K. Raghavachari, J.B. Foresman, J.V. Ortiz, Q. Cui, A.G. Baboul, S. Clifford, J. Cioslowski, B.B. Stefanov, G. Liu, A. Liashenko, P. Piskorz, I. Komaromi, R.L. Martin, D.J. Fox, T. Keith, M.A. Al-Laham, C.Y. Peng, A. Nanayakkara, M. Challacombe, P.M.W. Gill, B. Johnson, W. Chen, M.W. Wong, C. Gonzalez, J.A. Pople, Gaussian-03 suite of programs, Gaussian, Inc., Pittsburgh, PA, 2003.

[30] (a) J.J.P. Stewart, J. Comp. Chem. 10 (1989) 209–220;
(b) J.J.P. Stewart, J. Comp. Chem. 10 (1989) 221–264.

[31] (a) A.E. Reed, R.B. Weinstock, F. Weinhold, J. Chem. Phys. 83 (1985) 735–746;
(b) A.E. Reed, F. Weinhold, L.A. Curtiss, Chem. Rev. 88 (1988) 899–926.

[32] R.F.W. Bader, Chem. Rev. 91 (1991) 893–928.

[33] F. Biegler-König, J. Schönbohm, D. Bayles, J. Comp. Chem. 22 (2001) 545–559.

[34] (a) K. Wang, M. Lu, A. Yu, X. Zhu, Q. Wang, J. Org. Chem. 74 (2009) 935–938;
(b) C. Coperet, Chem. Rev. 110 (2010) 656–680.

[35] (a) G.C. Stocco, A. Tamburello, M.A. Girasolo, Inorg. Chim. Acta. 78 (1983) 57–61;
(b) W. Levason, C.A. McAulefee, G.S.G. Murray, J. Chem. Soc. Dalton Trans. (1975) 1566–1570;
(c) D.L. Lewis, E.D. Estes, D.J. Hodgson, J. Cryst. Mol. Struct. 5 (1975) 67–74.

[36] (a) A. Sharifi, M. Mirzaei, M.R. Nami-Jamal, Monatsh. Chem. 137 (2006) 213–217;
(b) Z. Li, S. Bohle, C.-J. Li, Proc. Natl. Acad. Sci. 103 (2006) 8928–8933;
(c) D. Cheng, W. Bao, J. Org. Chem. 73 (2008) 6881–6883;
(d) Y. Zhang, C.-H. Li, Angew. Chem. Int. Ed. 45 (2006) 1949–1952.

[37] J. Kamlet, J.-L.M. Abboud, M.H. Abraham, R.W. Taft, J. Org. Chem. 48 (1983) 2877–2887.

[38] Absorption spectral changes of **2** as a function of pH were studied in $CH_3CN:H_2O$ (1:1, *v*/*v*). As shown in the Supporting Information (Fig. S4), **2** was found to be stable within a pH range 1-7 thus the determination has been performed using HEPES buffer. Also it was found that using Tris buffer, detection of Hg^{2+} by **2** was also feasible (Fig. S5 in Supporting Information).

[39] J. Huang, Y. Xu, X. Qian, J. Org. Chem. 74 (2009) 2167–2170.

[40] (a) C.J. Webb, L.M. Clark, B. Carson, K. Helf, M. Ruck, S. Dawadi, Philadelphia Annual Meeting, 2006;
(b) K. Bischoff, J. Pichner, W.E. Braselton, C. Counard, D.C. Evers, W.C. Edwards, Arch. Environ. Contam. Toxicol. 42 (2002) 71–76.

[41] (a) F.A. Carey, Organic Chemistry, 4th edn, McGraw Hill, 2000;
(b) C. Gallina, M. Maneschi, A. Romeo, J. Chem. Soc. Perkin Trans. 1 (1973) 1134–1136.

[42] The reported distance between mercury and carbon in a covalent bond should be of the order of 2.075 Å as in the X-ray crystal structure of [MeHg([9]aneS_3)] + [43]. This distance is slightly overestimated by the B3LYP/LanL2DZ method (2.237 Å).

[43] M. Wilhelm, S. Deeken, E. Berssen, W. Saak, A. Lutzen, R. Koch, H. Strasdeit, Eur. J. Inorg. Chem. (2004) 2301–2312.